Applied Surface Science 257 (2011) 3374–3377

Contents lists available at ScienceDirect

Applied Surface Science

journal homepage: www.elsevier.com/locate/apsusc

Surface reconstruction of ZnO nanowire arrays via solvent-evaporation-induced self-assembly

Fang Fang[a,*], Dongxu Zhao[b,**], Binghui Li[b], Zhenzhong Zhang[b], Dezhen Shen[b], Xiaohua Wang[a]

[a] Changchun University of Science and Technology, 7089 Wei-Xing Road, Changchun 130022, People's Republic of China
[b] Key Laboratory of Excited State Processes, Changchun Institute of Optics, Fine Mechanics and Physics, Chinese Academy of Sciences, 16 East Nan-Hu Road, Open Economic Zone, Changchun 130033, People's Republic of China

ARTICLE INFO

Article history:
Received 27 April 2010
Received in revised form 2 November 2010
Accepted 4 November 2010
Available online 16 November 2010

Keywords:
Zno nanowires
Self-assembly

ABSTRACT

Vertically aligned ZnO nanowires (NWs) can be reconstructed on large scales by a solvent-evaporation-induced method. The morphologies of the nanowires are regulated by changing the concentration of the solution. Possible mechanism, which the compressive residual stresses and wires/wires self-attraction can be responsible for the surface reconstruction, is addressed. Furthermore, we compare the structural properties of ZnO nanowires before and after reconstructed.

1. Introduction

Large-scale and controlled arrays of nanostructures are key components for the manufacturing of nanodevices. A lot of researches are attached on the discovery and development of new nanoscale structures with an emphasis to control accurately in morphology, size and structure, because these characters will define and control the physical and chemical properties. Since it is difficult to manipulate the morphology of the fabricated nanostructures at large scales, most of these researches are focus on the control over the nanostructures during the growth process [1–6]. The morphological deformation of one dimensional nanostructures such as silicon nanocolumns could be reversely actuated by hydrogel which swells and contracts depending on the humidity level [7]. Based on the remarkable physical properties of nanoscale zinc oxide, such as semiconducting, piezoelectric (PZ), mechanical and biocompatible properties, ZnO NWs were attracted much attention recently. A variety of functional devices based on ZnO nanostructures, such as gas and chemical sensors, ultraviolet lasers, light-emitting diodes (LEDs), photodetectors, and piezoelectric nanogenerators have been fabricated [8–12]. In this letter, we present here a facile approach with large scale processing capability to reconstruct ZnO nanowire arrays via a solvent-evaporation-induced process.

2. Experimental

The ZnO NWs used in our experiments were fabricated via a simple vapor-phase transport process on Si (0 0 1) substrate in a horizontal tube furnace described previously [13]. A mixture of commercial ZnO and graphite powders in a certain weight ratio (1:1) was loaded in a quartz boat served as source material. Synthesis was carried out at 990 °C under a constant flow of Ar (99.99%) with the flow rate of 100 sccm for 30 min. The Si substrate was laid above the source material with a vertical distance of 4 mm. A thin layer of ZnO was deposition on Si surface by electron beam evaporation method with the thickness of 70 nm which used as the nucleation template and also control the growth direction of ZnO nanowires. After deposition a white gray layer was found on the ZnO thin film/Si substrate surface. Field-emission scanning electron microscopy shows that the as-grown nanowires are well-aligned along the normal direction of the substrate. The as-grown samples are vertically oriented, uniform nanowires with diameter $d = 100–200$ nm, height $h = 10–13$ μm, and aspect ratios $h/d = 50–130$ (as shown in Fig. 1).

Poly(N-vinylcarbazole) (PVK) is a hole transport organic semiconducting polymer. It has been widely used as an electronic and optical material. After tried several polymers and solvents based on their solubility and compatible properties, PVK and chloroform were chosen. The commercial PVK powders were sonicated in chloroform for 1 h at room temperature with three different

---

* Corresponding author at: Changchun University of Science and Technology, Department of Physics, 7089 Wei-Xing Road, Changchun, People's Republic of China. Tel.: +86 431 86176322; fax: +86 431 4627031.
** Co-Corresponding author at: Key Laboratory of Excited State Processes, Changchun Institute of Optics, Fine Mechanics and Physics, Chinese Academy of Sciences, 16 East Nan-Hu Road, People's Republic of China.
E-mail addresses: fangfang1982131@yahoo.com.cn (F. Fang), dxzhao2000@yahoo.com.cn (D. Zhao).

0169-4332/$ – see front matter © 2010 Elsevier B.V. All rights reserved.
doi:10.1016/j.apsusc.2010.11.027

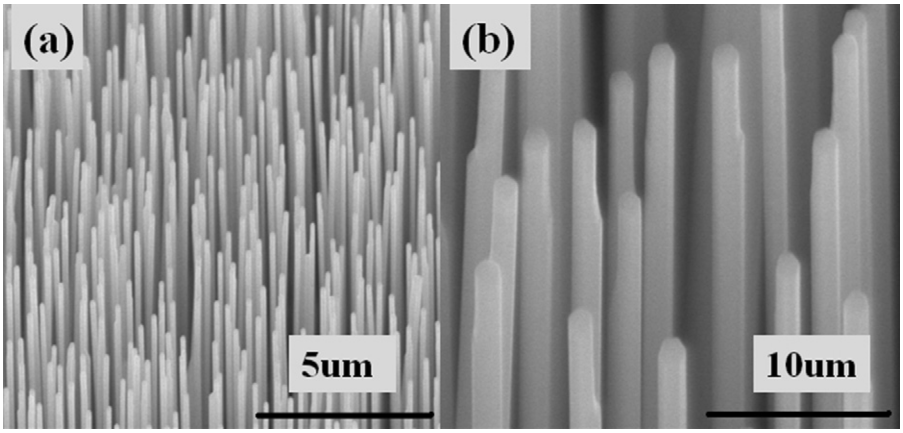

Fig. 1. FESEM images of the as-grown ZnO NW arrays on ZnO film/Si (0 0 1) substrate (with different magnification (a) and (b)).

concentrations (A: 10 mg/mL, B: 20 mg/mL and C: 30 mg/mL). By dripping the macromolecular solution on the surface of the NW arrays, the morphologies of the vertically aligned ZnO NWs were bended during the solvent-evaporation process.

3. Results and discussion

The morphology of NWs varied with different PVK concentrations was monitored by the field-emission scanning electron microscopy (FESEM) (as shown in Fig. 2). The SEM image reveals that the adjacent NWs attach together as a result of polymer shrinkage in lower concentration (10 mg/mL, here is labeled sample A shown in Fig. 2(a)). A honeycomblike pattern on the surface controls the formation of a complex structure in arrays of perpendicular oriented NWs by increasing the concentration of solution to 20 mg/mL (labeled sample B, Fig. 2(b)). With the increasing of solution concentration, more polymer remains on the sample surface. The fracture can be seen from the root of some NWs in each comb (see the white circle in the inset image of Fig. 2(b)) due to the large deflections. The cleavage plane perpendicular to the NWs axis, that is, parallel to the (0 0 0 1) planes [14]. Since the observation of the NWs is made particularly difficult by the presence (and thickness) of the polymer, which strongly reduces the image contrast [15]. The largest concentration of solution (30 mg/mL, labeled sample C) makes the polymer layer thick enough to cover the whole surface of the NWs. And there are no clear images shown here. We found that the PVK polymer residues on the top end of the NWs played an important role in providing structure support to the ZnO NWs.

Trying to remove the effect of the polymer, the samples were rinsed in pure chloroform solvent to dissolve the PVK residues. As shown in Fig. 3(a), the morphology of the sample A did not change after rinsing process (the inset image verified that there was nothing left in the ZnO NWs), even after the annealing treatment at 700 °C for 1 h in air or deposited in air for 30 days. The similar case appears on other samples, in addition to the broken NWs dispersed on the sample surface which is due to the absence of polymer support (Fig. 3(b)). Especially for the sample C, a large amount of fractured NWs can be seen on the substrate (not shown here). Since there was no strenuous vibration used in the rinsing process, we deduce this broken phenomenon must occur before rinsing due to large stress may generated from polymer shrinkage in largest concentration of the solution (30 mg/mL).

According to preliminary results shown here, we suggest the surface reconstruction phenomenon observed is due to: (i) compressive residual stresses resulting from polymer shrinkage during the solvent-evaporation process, and (ii) wires/wires self-attraction when the bended NWs attached each other. Regarding hypothesis (i) above, the applied stress is transferred to the NWs via a polymer chains twisting process. With the increased nanowire-polymer affinity, the macroscopic stress transferring phenomena are dominant [16]. Based on our previous report [17], the as-grown ZnO NW arrays interface are hydrophobicity. This result is further confirmed by contact angle measurements, in which the PVK-chloroform solution filled ZnO NW arrays exhibited a contact angle less than 15°. Therefore, it is much easier for PVK chains to twist the whole nanowires and fill in the interspace of nanowires. Because of the low boiling point of chloroform solvent (60 °C), the evaporating process of solvent was fast and the polymer PVK was left on ZnO NWs. The compressive residual stresses resulting from polymer shrinkage transferred to the NWs via polymer cohesion process, which leads to the bending of nanowires. Meanwhile, with the increasing of concentration, the stresses transfer from polymer to NWs may be sufficiently large to fracture some NWs due to the large deflections. The apparent bending angles measured from the SEM images range from 20° to 50°, with a majority of the angles centered around 20–30° in sample A. The largest bending angle in sample B is about 50° (the actual values may deviate due to the uncertainties in the exact NWs tilting angle with respect to the electron beam). Here, we suggest that the residual strain resulting from polymer shrinkage may contribute to the permanent deformation and fracture of NWs (especially, in higher concentration). However, in our knowledge, many researches [6,13,18] on the bending strength and flexibility of ZnO materials indicated that such bending angles shown in our experiment (in sample A) cannot form plastic deformation. Recently, Wang's group observed the dense well-aligned epitaxial ZnO nanorod bundles to be self-attracted after preparation for 20 days [19]. Although the bending feature in virtue of self-attraction between the ZnO nanorods is not clear yet, this phenomenon has been verified. Therefore, we deduce that the solvent-evaporation process may accelerate the self-attraction process. Even if we rinsed the polymer, the wires/wires self-attractions cannot be released. We deduce that both hypothesizes mentioned above are all responsible for the surface reconstruction. In addition to other structural parameters, such as aspect ratios h/d or the area density of the NWs, cannot be negligible. The higher aspect ratios and area density are, the easier the deflection of the NWs occurs in our experiment. The mechanism of the bending properties is still under investigation.

Furthermore, we characterized the structural properties of as-grown ZnO NWs and bended ZnO NWs (rinsed sample A). Fig. 4 shows the X-ray diffraction (XRD) spectra of the as-grown ZnO NWs and bended ZnO NWs. Both samples are c-axis preferred orientation, which can be confirmed by only ZnO (0 0 2) diffractive peak appeared in the spectra. In contrast to the as-grown ZnO NWs, the

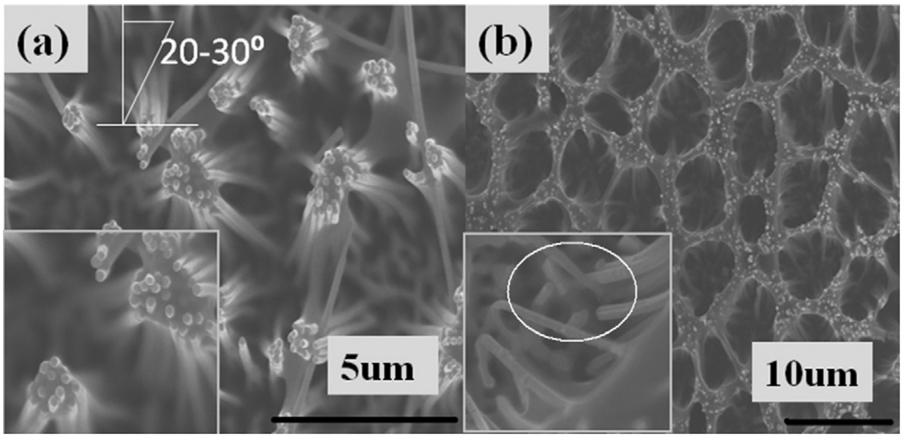

Fig. 2. FESEM images of the ZnO NW arrays after dripping the macromolecular solution on the surface with different concentrations (a) for sample A, 10 mg/mL, (b) for sample B, 20 mg/mL (the inset images shown at high magnification).

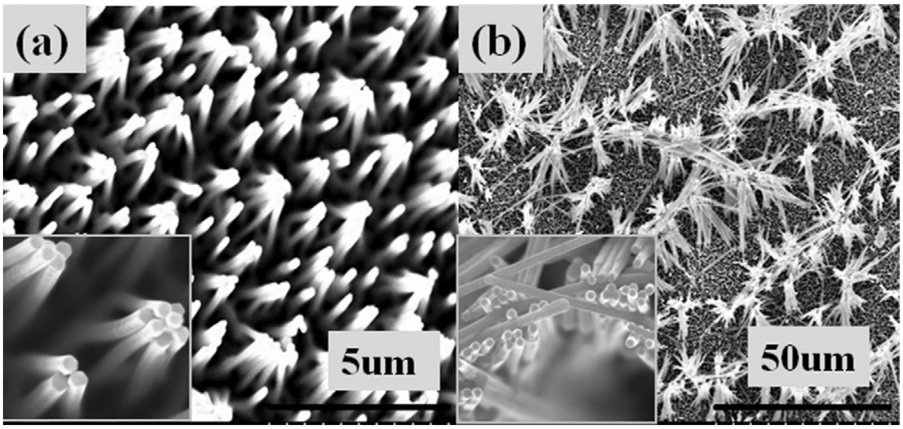

Fig. 3. FESEM images of the ZnO NW arrays after rinsing the PVK residues (a) for sample A, (b) for sample B (the inset images shown at high magnification).

bended NWs have a weaker intensity of (0 0 2) diffractive peak. Obviously, the PVK treatment deteriorates the well-aligned orientation of as-grown ZnO NWs. Meanwhile, compared the (0 0 2) diffractive peak position of as-grown ZnO NWs($2\theta = 34.52^\circ$) with bended one($2\theta = 34.45^\circ$), the (0 0 2) positions have a little deviation. It is suggested that there may be some residual strain in bended ZnO NWs during the reconstruction process.

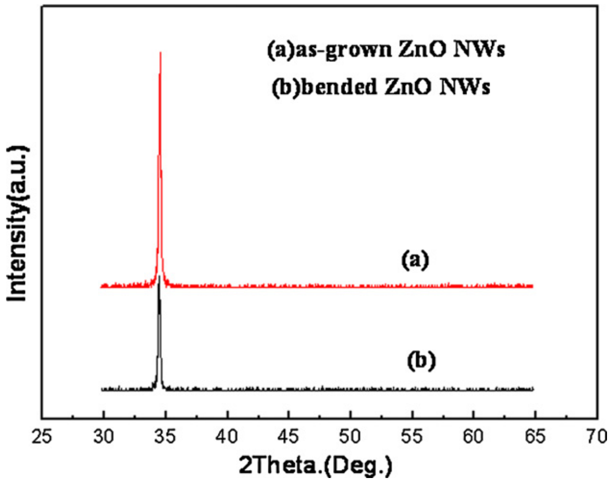

Fig. 4. XRD results of: (a) as-grown ZnO NWs and (b) bended ZnO NWs (rinsed sample A).

Fig. 5 shows resonance Raman scattering spectra for (a) as-grown ZnO NWs and (b) bended ZnO NWs at room temperature. The first-order LO modes of ZnO resonance Raman peaks are measured to be 570 cm^{-1}. Compared to as-grown sample, the position of LO mode nearly maintained unchanged, but bended ZnO NWs have stronger Raman signals. The vibration orders of ZnO resonance Raman peaks are also increased from 4 orders to 5 orders accompanied with bandwidth broadening (inset of Fig. 5). The phenomena

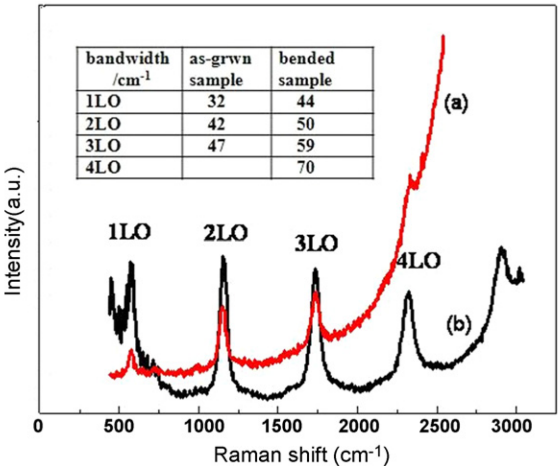

bandwidth /cm^{-1}	as-grwn sample	bended sample
1LO	32	44
2LO	42	50
3LO	47	59
4LO		70

Fig. 5. Resonance Raman spectra of: (a) as-grown ZnO NWs and (b) bended ZnO NWs excited with 325 nm He–Cd laser.

of enhancing the Raman signals have been observed in multiple-quantum-well and superlattices structures [20,21]. Such Raman process is due to Frohlich-interaction electron–phonon scattering activated by the strain-generated electric fields that occur in the multiple-quantum-well structures. To the wurtzite structure crystals, stress induced in the crystals affected the E_2 (high) phonon frequency obviously [22]. In our experiment the weak peak around 437 cm^{-1}, which was contributed to the E_2 (high) mode, was almost imperceptible in as-grown ZnO NWs compared with other (overlapping/stronger) resonance Raman scattering peaks. However, we could also deduce that strain present in the ZnO NWs because of the Raman phonon bandwidth broadening [23], which further validates the above speculation for residual stresses.

4. Conclusions

In summary, it is demonstrated that the original vertically aligned ZnO nanowire arrays can be large-scale reconstructed into different morphologies via a simple solvent-evaporation process. The compressive residual stresses and wires/wires self-attraction can be responsible for the deformation. It enables the morphological alteration after the growth process on large scales to be realized. In addition to its patterning benefits, there are a number of additional advantages associated with the present method. Such solvent-evaporation-induced self-assembly nanocomposites (consisting of inorganic nanoparticles and organic polymers) are supposed to exhibit a host of optical, electrical, and magnetic properties, which are far superior compared with those of the individual components. And that, if we choose the biopolymer solution and ZnO nanostructures (also biocompatible materials) which will widen the scope of application to biomedicine further.

Acknowledgments

This work is supported by the National Natural Science Foundation of China (61006065 and 61076039), the Program for New Century Excellent Talents in University (NCET-07-022), the Project of Science Development Planing of Jilin Province (20080331-1, 20090139, and 20090555), the Natural Science Foundation of Jilin Province (20101546), and Department of Education of Jilin Province [2008] 296. Quality Project of Changchun University of Science (2009A0102.2009B0107).

References

[1] D.J. Sirbuly, M. Law, J. Yan, P. Yang, J. Phys. Chem. B 109 (2005) 15190–15193.
[2] X.L. Wang, H. Zhu, Z.J. Wang, F. Yang, X.R. Yang, Chem. Eur. J. 15 (2009) 11473–11477.
[3] R.S. Yang, Y. Ding, Z.L. Wang, Nano Lett. 4 (2004) 1309–1314.
[4] X.Y. Kong, Z.L. Wang, Appl. Phys. Lett. 84 (2004) 975–979.
[5] W.L. Hughes, Z.L. Wang, J. Am. Chem. Soc. 126 (2004) 6703–6705.
[6] W.L. Hughes, Z.L. Wang, Appl. Phys. Lett. 86 (2005) 043106–043109.
[7] A. Sidorenko, T. Krupenkin, A. Taylor, P. Fratzl, J. Aizenberg, Science 315 (2007) 487–491.
[8] Z.W. Pan, Z.R. Dai, Z.L. Wang, Science 291 (2001) 1947–1951.
[9] Z.L. Wang, J.H. Song, Science 14 (2006) 242–245.
[10] S. Xu, C.S. Lao, B. Weintraub, Z.L. Wang, J. Mater. Res. 23 (2008) 2072–2075.
[11] X.L. Wang, H. Zhu, Z.J. Wang, F. Yang, X.R. Yang, Chem. Eur. J. 15 (2009) 4253–4257.
[12] F. Fang, D.X. Zhao, B.H. Li, Z.Z. Zhang, D.Z. Shen, Phys. Chem. Chem. Phys. 12 (2010) 6759–6761.
[13] F. Fang, D.X. Zhao, J.Y. Zhang, D.Z. Shen, Y.M. Lu, X.W. Fan, B.H. Li, X.H. Wang, Nanotechnology 18 (18) (2007) 235604–235609.
[14] C.Q. Chen, J. Zhu, Appl. Phys. Lett. 90 (2007) 1043105–1043107.
[15] H.D. Wagner, O. Lourie, Y. Feldman, R. Tenne, Appl. Phys. Lett. 72 (1998) 188–190.
[16] D.W. Chae, B.C. Kim, Polym. Adv. Technol. 16 (2005) 846–850.
[17] X.Q. Meng, D.X. Zhao, J.Y. Zhang, D.Z. Shen, Y.M. Lu, L. Dong, Z.Y. Xiao, Y.C. Liu, X.W. Fan, Chem. Phys. Lett. 413 (2005) 4–9.
[18] S. Hoffmann, F. Östlund, J. Michler, H.J. Fan, M. Zacharias, S.H. Christiansen, C. Ballif, Nanotechnology 18 (2007) 205507–205512.
[19] X.H. Han, G.Z. Wang, L. Zhou, J.G. Hou, Chem. Commun. (2006) 212–216.
[20] I. Sela, D.L. Smith, Phys. Rev. B46 (1992) 1480–1484.
[21] G. Rozas, M.F. Pascual Winter, A. Fainstein, B. Jusserand, P.O. Vaccaro, S. Saravanan, Phys. Rev. B 77 (2008) 165314–165319.
[22] H.-M. Cheng, H.-C. Hsu, Y.-K. Tseng, L.-J. Lin, W.-F. Hsieh, J. Phys. Chem. B 109 (2005) 8749–8752.
[23] H.T. Ng, B. Chen, J. Li, J. Han, M. Meyyappan, Appl. Phys. Lett. 82 (2003) 2023–2025.